Nuclear Engineering and Technology 53 (2021) 3704–3710

Contents lists available at ScienceDirect

Nuclear Engineering and Technology

journal homepage: www.elsevier.com/locate/net

Original Article

Change in radiation characteristics outside the SNF storage container as an indicator of fuel rod cladding destruction

V.G. Rudychev [a], N.A. Azarenkov [a], I.O. Girka [a], Y.V. Rudychev [a, b, *]

[a] V.N. Karazin Kharkiv National University, 4 Svobody Sq., Kharkiv, 61022, Ukraine
[b] National Science Center Kharkiv Institute of Physics and Technology, 1, Akademicheskaya St., Kharkiv, 61108, Ukraine

ARTICLE INFO

Article history:
Received 30 December 2020
Received in revised form
27 April 2021
Accepted 22 May 2021
Available online 1 June 2021

Keywords:
Storage container
Fuel rod claddings
Dry cask storage

ABSTRACT

The characteristics of the external radiation on the surface of the casks for spent nuclear fuel (SNF) storage by dry method are investigated for the case when the spatial distribution of SNF in the basket changes due to the destruction of the fuel rod claddings. The surface areas are determined, where the changes in fluxes of neutrons, produced by ^{244}Cm actinide, and γ-quanta, produced by long-lived isotopes, are maximum in the result of the decrease in the height of the SNF area. Concrete (VSC-24) and metal (SC-21) casks are considered as examples. The procedure of periodic measurement of the dose rate of neutrons or γ-quanta at the specified points of the cask surface is proposed for identifying the fuel rod cladding destruction. Under normal operation, the decrease in the dose rate produced by neutrons as the function of SNF storage duration is determined by the half-life of ^{244}Cm, and for γ-quanta - by the half-lives of long-lived SNF isotopes. Consequently, a stepwise change in the dose rate of neutrons or γ-quanta, detected by the measurements, as compared to the previous one, would indicate the destruction of the fuel rod claddings.

1. Introduction

When storing spent nuclear fuel (SNF) by dry method, the technique of SNF storage in cask with cooling due to natural convection of environmental air is used. In the process of storage, the heat release decreases rather slowly with time. That is why, the spent fuel assemblies (SFAs) are stored at relatively high temperatures for a long time. Generally, the heat release power of one SFA from the WWER-type reactors is ~1 kW for SNF with the burnup level from 35 to 45 MW·day/kg U and cooling time of more than 5 years [1]. Such heat release provides the temperature of ~300 °C inside the basket with SFAs under normal operation for storage casks of different design [2]. In the course of the SNF long-term storage, the destruction of both the fuel rod claddings and the SFA spacer grid is possible with subsequent SNF spilling out to the bottom of the sealed storage basket. The interaction of SNF with the metal (steel) of the basket can destroy the latter and cause the release of radionuclides into the environment. At present, there are no techniques for monitoring the possible destruction of the claddings with subsequent SNF spilling to the bottom of the storage basket. Monitoring the temperature of the cask outlet air, and comparing it with the environment temperature does not make it possible to determine the change in the geometric configuration of the heat source, since it depends on the heat release of the entire SNF volume [3].

The objective of the present paper is to study the characteristics of the external radiation, caused by change in the radiation source shape, as a result of possible destruction of the fuel rod claddings and SNF spilling to the bottom of the sealed basket of the dry storage cask.

2. Simulation of the radiation source

In the present paper, the change in the external radiation caused by the variation of the SNF shape is investigated. Two types of the dry storage casks are considered: concrete VSC-24 [4] and metal SC-21 [5]. In the concrete storage cask VSC-24, 10 cm of steel and 70 cm of concrete serve as the radiation shielding from γ-quanta and neutrons emitted by 24 SFAs in the radial direction, see Fig. 1a. The radiation attenuation in the axial direction is ensured by 40 cm

* Corresponding author. National Science Center Kharkiv Institute of Physics and Technology, 1, Akademicheskaya St., Kharkiv, 61108, Ukraine.
E-mail address: erudychev@gmail.com (Y.V. Rudychev).

https://doi.org/10.1016/j.net.2021.05.029

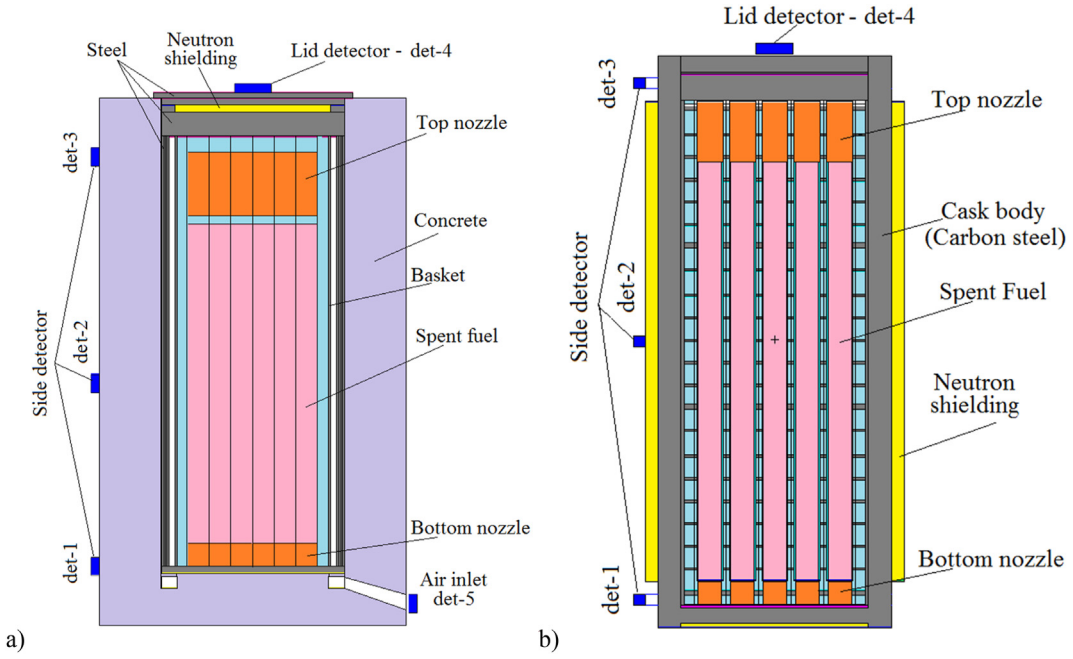

Fig. 1. (a) Schematic of the VSC-24 storage cask; (b) Schematic of SC-21 storage cask.

of steel and 5 cm of a neutron absorber, i.e. the plate made of RX-277 material. The composition of this material is as follows: B ~0.02, O ~0.61, Al ~0.25, Si ~0.02, Ca ~0.09.

The SC-21 storage cask comprises 21 SFAs. In this case, the shielding from γ quanta in the radial direction is ensured by ~25 cm of steel, and from neutrons – by ~11 cm of rubber, Fig. 1b. The radiation shielding in the axial direction is ensured by the lid of the basket with SNF, and the lid of the container. Both of them are made of steel ~40 cm thick.

The characteristics of γ-quanta and neutrons on the containers surfaces are calculated using the MCNP code [6]. The schematic of storage casks VSC-24 and SC-21, simulated in the MCNP code, with the radiation detectors arrangement taken into account, is presented in Fig. 1. The detectors, determining the radiation in the axial direction, are located on the weatherproof lid, and in the radial direction – on the container side surface at different heights. On the VSC-24 storage cask, the detectors are also located at the inlets of the air ducts.

For both the concrete and metal SNF storage casks, two options for the change of the radiation source configuration are considered. Option I is as follows. Only fuel rod claddings are destroyed, without any destruction of the SFA load-bearing elements, with further SNF spilling to the bottom of the storage basket. In this case, the top nozzles (indicated as TN in Fig. 2) remain in the upper position. Option II: the fuel rod claddings are destroyed along with the destruction of the SFA load-bearing elements with subsequent SNF spilling out to the bottom of the storage basket and displacement of the top nozzles down from the upper position (indicated as TNII in Fig. 2). Since the temperature of the central SFAs is higher [2], the probability of destruction of the fuel rod claddings in such assemblies is also higher. For the options I and II, the possibility of the fuel rod cladding destruction both for all 24 SFAs in VSC-24 (21 SFAs in SC-21), and for only 10 central SFAs in VSC-24 (9 SFAs in SC-21) is considered. In the latter case, the SNF characteristics of the fourteen SFAs in VSC-24 (12 SFAs in SC-21), located along the basket perimeter, are assumed to remain unchanged. The placement layout of SFAs in VSC-24 container for the four options described below are presented in Fig. 2. The radiation source is simulated in the form of three zones. The first one is the homogenized area of SNF (destroyed SFAs). The second one is the steel top nozzles. And the third one is the bottom nozzles.

For SC-21 cask, these options are indicated as: I-21, I-9 and II-21, II-9. Note, that when simulating radiation from each of the 24 SFAs for the VSC-24 WWER-1000 and radiation from the homogenized SNF zone, the calculation results for the external radiation (for both γ-quanta and neutrons) differ by only 2 or 3% [7].

3. Radiation sources

The radiation source in the VSC-24 storage cask is SNF with the initial fuel enrichment of 4.4%, burnup of 40.5 MW·day/t U after the three-year campaign in the WWER-1000 reactor and more than five years of cooling time in near-reactor cooling ponds.

3.1. Gamma radiation source

The main source of γ-quanta from SNF is the primary gamma radiation of fission products and long-lived actinides. The additional gamma radiation is generated by ^{60}Co, produced as a result of activation of the SFA steel elements containing ^{59}Co, as well as by γ-quanta generation in (n, γ) reactions on SNF fissile and non-fissile elements and on those of SFAs. Generally, the external radiation during dry storage of fuel for the given cooling time of SNF is calculated on the basis of the primary γ-quanta spectral composition, which depends on the type of fuel, its enrichment and burnup level. To analyze the changes in the external radiation characteristics subject to the SNF storage time, it is expedient to determine the radiation from individual isotopes with different half-lives. Note, that well-known parent beta-emitters for given γ-emitters are indicated here in brackets, for example ^{137m}Ba (^{137}Cs). The isotopes ^{90}Y (^{90}Sr), ^{106}Rh (^{106}Ru), ^{134}Cs, ^{137m}Ba (^{137}Cs), ^{144}Pr (^{144}Ce), ^{154}Eu, as well as ^{60}Co are known to make the maximum contribution to γ-radiation outside the container at storage times of more than five years [8]. Table 1 presents the basic characteristics of these isotopes: half-lives $T_{1/2}$; energies of γ-quanta, Eγ, whose quantum yields are more than 5% of the total yield, Y_i; and activity

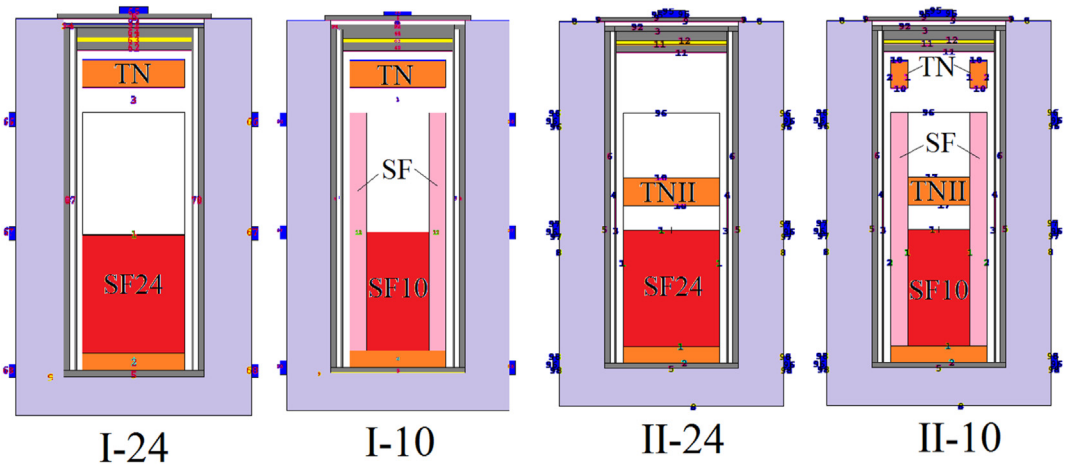

Fig. 2. Placement layout of SFAs in the VSC-24 cask for four options of destruction for both the fuel rod claddings and SFA load-bearing elements, generated in MCNP code.

Table 1
Characteristics of the basic isotopes and their quantum yields per 1 Bq.

Isotope	$T_{1/2}$ (year)	Eγ, MeV, (yield/1 Bq, > 5% total)	Y_{iz}, yield/1Bq, total (Eγ>0.2 MeV)	A_{iz}, activity, Bq/tU
^{60}Co	5.27	1.17 (0.999); 1.33 (0.9998)	2	
^{90}Y (^{90}Sr)	28.5	1.76 (0.00016)	0.00016	$3.26\cdot10^{15}$
^{106}Rh (^{106}Ru)	1.009	0.51 (0.207); 0.62 (0.106)	0.33	$3.02\cdot10^{15}$
^{134}Cs	2.06	0.57 (0.15); 0.60 (0.975); 0.8 (0.851)	2.224	$2.73\cdot10^{15}$
^{137m}Ba (^{137}Cs)	30	0.662 (0.9)	0.9	$4.15\cdot10^{15}$
^{144}Pr (^{144}Ce)	0.778	0.697 (0.013); 1.49 (0.0028); 2.19 (0.0071)	0.0235	$3.77\cdot10^{15}$
^{154}Eu	8.6	0.6 (0.061); 0.72 (0.2); 0.87 (0.115); 1.0 (0.28); 1.27 (0.355)	1.22	$3.86\cdot10^{14}$

A_i for cooling time in near-reactor cooling ponds of three years [9]. The contribution of γ-quanta from reactions (n, γ) to the external radiation is much smaller than that from the fission products and emitters with induced activity [5].

3.2. Neutron source

The Spontaneous fission of ^{244}Cm, whose half-life is 18.1 years, as well as ~0.8% of ^{240}Pu and ^{242}Pu are the main (about 97.4%) sources of neutrons produced in SNF [10].

The spectrum of the neutrons, produced by the spontaneous fission of actinides, is similar to that from the induced fission of ^{235}U, and is approximated by the following expression:

$$N(E) = \frac{2\sqrt{E}}{\sqrt{\pi\theta^3}}\exp(-E/\theta), \quad (1)$$

where E is energy, MeV, and θ is the hardness parameter, equal to 1.33 MeV for ^{244}Cm [11]. The average energy of such neutrons is approximately 1.995 MeV. The neutron yield from all 24 SFAs, loaded into the cask for SNF with the burnup of 40.5 MW·day/t U and cooling time of 3 years is about 3.76×10^9 neutrons/s.

4. Results of calculating the external radiation characteristics

4.1. Neutrons

The radiation shielding of storage casks VSC-24 and SC-21 in the radial and axial directions differ significantly for neutrons and γ-quanta. In the VSC-24 container, the neutron flux in the radial direction is significantly attenuated by radiation shielding, made of 70-cm thick concrete. The neutron dose rate D_n on the cask side surface is by the order of magnitude lower than gamma dose rate D_γ. For example, for VSC-24 cask, $D_n \approx 0.8$ mSv/h, and $D_\gamma \approx 30$ mSv/h [4]. For the metal storage cask of the SC-21 type [5] with neutron shielding made of different materials, the dose rates on the cask side surface in the radial direction are approximately equal for γ-quanta and neutrons, $D_n \approx D_\gamma$. The radiation shielding in the axial direction in storage casks VSC-24 and SC-21 is ensured by steel ~40 cm thick. As the result, the attenuation of the neutron flux in the axial direction is lower than that of γ-quanta. Therefore, for the VSC-24 container, $D_n \approx 82$ μSv/h, and $D_\gamma \approx 19$ μSv/h [4].

The neutron spectra, emitted by ^{244}Cm from the SNF zone on the surface of the VSC-24 and SC-21 storage casks, are calculated using the MCNP code. The spectra of primary neutrons of ^{244}Cm isotope (curve Sp_W) on the weatherproof lid of VSC-24 storage cask (curve VSC-24_Lid) and on the side surfaces of VSC-24 and SC-21 storage casks (curves VSC-24_Side and SC-21_Side) are shown in Fig. 3. The data presented in Fig. 3 illustrate significant decrease in the energy of high-energy neutrons after passing through radiation shielding made of concrete (VSC-24) or rubber (SC-21).

The neutron dose rates D_{norm} on the VSC-24 weatherproof lid to be registered in det-4 detector under normal operation, as well as the neutron dose rate D at destruction of 1/6, 1/3 and 1/2 of the fuel rods are calculated for Option I-24. The ratio D/D_{norm} is indicated in Fig. 4 by triangles. For Option I-24 (destruction of all 24 SFAs), the height of the entire radiation source as a whole, decreases. This leads to the significant decrease in D/D_{norm} to the value of ≈0.7 already for the case of 1/6 of the destroyed fuel rods. In Option I-10 (destruction of 10 central SFAs), the shape of the radiation source transforms to that of a thick-walled cup. In this case, D practically does not differ from D_{norm}, $D/D_{norm} \approx 1$, the respective curve is indicated by rectangles in Fig. 4. The magnitudes of the mean-

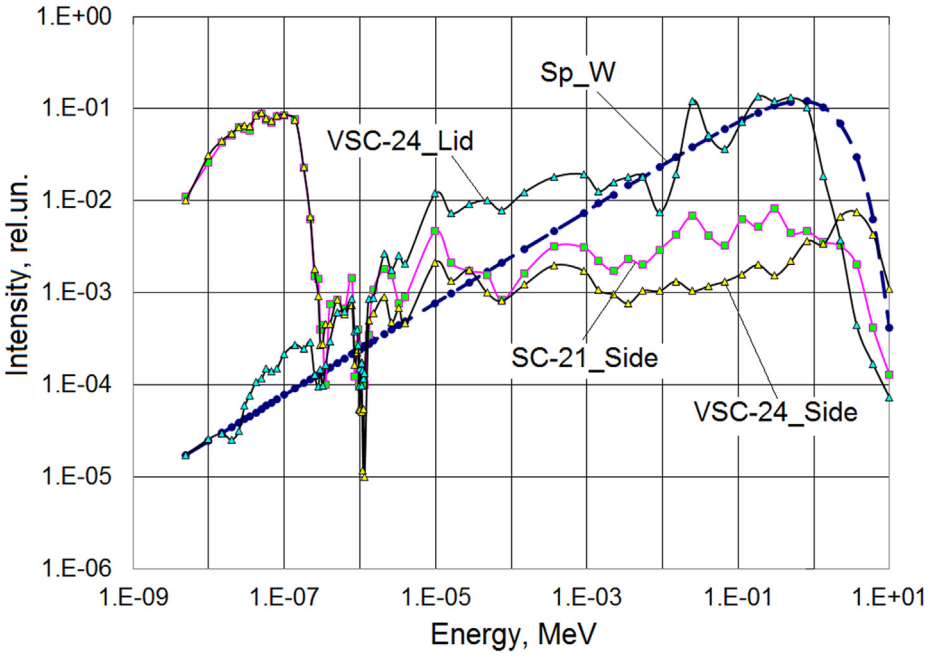

Fig. 3. Spectra of primary neutrons of ^{244}Cm isotope (curve Sp_W), on the weatherproof lid of VSC-24 cask (curve VSC-24_Lid) and on the side surfaces of VSC-24 and SC-21 storage casks (curves VSC-24_Side and SC-21_Side).

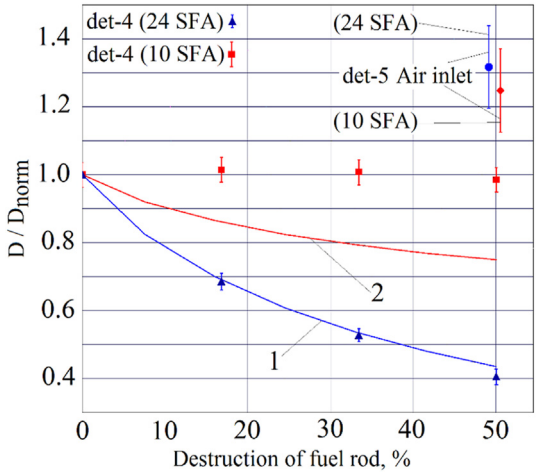

Fig. 4. Dependences of the ratio of the neutron dose rate D/D_{norm} on the fraction of the destroyed fuel rods.

square errors of the D/D_{norm} ratios, also presented in Fig. 4, make less than 3% for the det-4 detector, and less than 10% for the det-5 detector.

The simple model for calculating the radiation flux on the surface of objects, similar to options I-24 and I-10, due to the change in the source height, was proposed in [12]. The method of integration of point radiation sources without absorption, both in the source itself and in the shielding, was used. The dependences of D/D_{norm} on the fraction of destroyed fuel rods, caused only by the change in the height of the sources is presented in Fig. 4 [12]. The curve 1 corresponds to Option I-24, and the curve 2 corresponds to Option I-10. Thus, when the height of the entire radiation source (I-24) changes, the neutron dose rate on the weatherproof lid of VSC-24 storage cask, calculated in the MCNP code with the absorption in the source and in the shielding of the cask taken into account, see

Table 2
Magnitudes of D/D_{norm} in the locations of the detectors det-1, det-2, det-3, and det-4 at destruction of 25% and 50% of fuel rods in all 21 SFAs and in 9 central SFAs of the SC-21 storage casks.

Assembly destroyed	21 SFA		9 SFA	
Destruction of rod, %	25%	50%	25%	50%
D/D_{norm} (det-1)	1.14	1.38	1.02	1.11
D/D_{norm} (det-2)	1.10	0.45	1.03	0.98
D/D_{norm} (det-3)	0.34	0.16	0.95	1.03
D/D_{norm} (det-4)	0.35	0.18	1.41	1.51

the curve marked by triangles in Fig. 4, is practically determined by the source shape. When the radiation source has a thick-wall cup shape (I-10), the neutron dose rate on the VSC-24 weatherproof lid practically does not change (curve 2), despite the changes in the particle flux from a source with non-absorbing properties.

The changes in the neutron dose rates D on the side surface of the storage cask, calculated for options I-24 and I-10, practically do not differ from D_{norm}, $D/D_{norm} \approx 1$. The dose rates are calculated in the location of the detectors det-1, det-2, and det-3. The D/D_{norm} values in the location of the detector det-5 (cask air duct) for options I-24 and I-10 are shown in Fig. 4.

For the SC-21 cask, the calculations of the neutron dose rates on its side surface (in the locations of the detectors det-1, det-2, and det-3) and on the lid (det-4) are carried out for the case, when the SNF zone changes in accordance with options similar to I-24 and I-10. Table 2 presents the D/D_{norm} magnitudes for the locations of three detectors on the cask surface and one on its lid with 25% and 50% fuel rod destruction in all 21 SFAs and in 9 central SFAs. The magnitudes of the mean-square errors in determining the dose rate ratios, presented in Table 2, make less than 1% for the location of the det-1 detector, and about 5% for the rest of the detectors.

As it follows from the data shown in Fig. 4, the measurement of the neutron dose rate on the weatherproof lid of the VSC-24 cask is reliable for determining the change in the height of the SNF zone caused by the possible destruction of the fuel rod claddings of all 24

SFAs (I-24). When the fuel rod claddings of only 10 central SFAs of the VSC-24 cask (thick-wall cup) are destroyed (Option I-10), the dose rate changes with a sufficient degree of certainty in the VSC-24 air duct of storage cask. Therefore, the measurement of the dose rate in the VSC-24 air duct allows determining the change in the source shape, caused by possible 50% destruction of the fuel rod claddings of 10 central SFAs, with the accuracy of ~5%.

For the SC-21 cask, the possibility to determine the change in the source configuration under destruction of the fuel rod claddings of all 21 SFAs is shown, when using the det-4 detector on the cask lid (see Table 2). The design features and materials of the SC-21 shielding are shown to lead to an increase in the dose rate (see Table 2) measured in the locations of the det-4 detector in the case of possible destruction of 9 central SFAs ("thick-wall cup" Option).

The periodic (once or twice a year) measurements of the neutron dose rate on the weatherproof lid of the VSC-24 cask under normal operation of the SNF dry cask storage facility would show an exponential decrease in the D in accordance with the half-life of ^{244}Cm being 18.1 years. Deviation of the measured value of the dose rate from that expected on the basis of the previous measurements was shown in [13] to indicate the destruction of the fuel rod claddings.

In the following, the scenario is considered, in which 10 central SFAs in the VSC-24 cask are destroyed after 10 years of SNF storage, and the remaining 14 SFAs are destroyed after the next 5 years. The corresponding dependences of the dose rates, produced by neutrons on the weatherproof lid and in the air duck of VSC-24 on SNF storage time under normal operation and at the fuel rod cladding destruction are shown in Fig. 5. One can see that during the first nine years the values of the dose rate, produced by neutrons, correspond to the exponential decrease in the SNF neutron flux. The dose rate magnitude, measured on the tenth year of SNF storage, shows its stepwise increase in the VSC-24 air duck with no change in the dose rate, measured on the weatherproof lid. On the 15th year of SNF storage, there is a stepwise decrease in the neutrons dose rate produced on the weatherproof lid, and its increase in the VSC-24 air duct. Judging by the data in Fig. 5, such deviations of the dose rate from the exponential decrease definitely indicate the change in the SNF configuration.

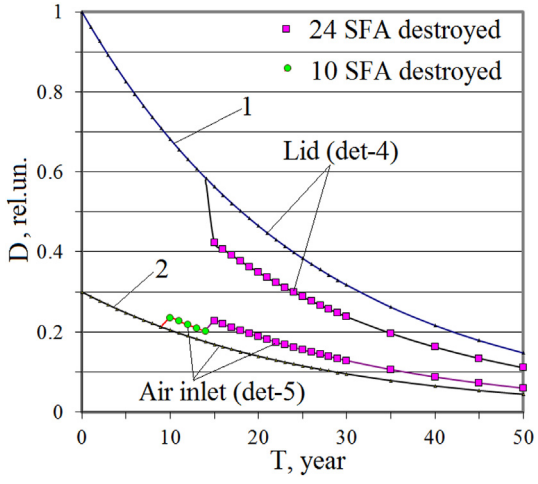

Fig. 5. Expected SNF storage time dependences of the neutron dose rate on the weatherproof lid (curve det-4) and in the air duck of VSC-24 under normal operation and at the fuel rod cladding destruction (indicated by squares for 24 SFA and by circles for 10 SFA).

4.2. Gamma quanta

In contrast to the neutron source, the source of γ-quanta is not only the SNF zone, but also the top nozzles and bottom nozzles of SFAs. The external radiation on the side surface of the storage cask is determined by those SFAs, which are located along the SNF zone perimeter. The emission of γ-quanta, in contrast to that of neutrons, is determined by isotopes with half-lives from ~0.8 to 30 years (see Table 1). Therefore, in the course of SNF storage for several years or even tens of years, the concentration of isotopes and their contribution to the external radiation change significantly.

In the axial direction, the additional shielding from SNF γ-quanta is provided by SFA top nozzles. This leads to the fact that the dose rate from γ-emitters of SNF on the weatherproof lid is much smaller than that on the side surface. Table 3 presents the magnitudes of the gamma dose rates D per source particle from the main SNF isotopes on the side surface of VSC-24 (in the location of det-2) and SC-21 (in the location of det-1) storage casks under normal operation and at 50% destruction of the fuel rods for options I- 24 (I-21) and I-10 (I-9).

Table 4 presents the magnitudes of the gamma dose rate, produced by ^{60}Co isotope contained in the SFA top nozzles, measured in the ring detectors (det-3) of VSC-24 and SC-21 storage casks, under normal operation and at 50% destruction of the fuel rods for options II-24 (II -21) and II-10 (II-9).

The total gamma doses ratios $D(T)/D(T)_{norm}$ of the six main isotopes for options I-24 and II-10 of storage cask VSC-24 (det-2) and for options I-21 and II -9 of SC-21 storage cask (det-1) versus the SNF storage time are shown in Fig. 6. The difference between the given dependences $D(T)/D(T)_{norm}$ for VSC-24 and SC-21 storage casks is caused by the difference in biological shielding of concrete and metal storage casks. Therefore, the contribution of each SNF isotope to the total dose on the cask surface is different for VSC-24 and SC-21. The contributions of individual isotopes to the dose rate for storage casks VSC-24 (det-2) and SC-21 (det-1) subject to the SNF storage time under normal operation are shown in Fig. 7.

The dependences of the dose rates on the SNF storage time are presented in Fig. 8. The change in the radiation dose rate on the surfaces of VSC-24 and SC-21 storage casks is determined by the change in the contributions of individual isotopes subject to the storage time of SNF, shown in Fig. 7a and b, respectively**.** It is assumed that 50% of the fuel rod claddings are destroyed between the ninth and tenth years of storage. This leads to the change in the SNF zone shape, to the consequent stepwise change in the dose rate on the cask surface, and to further decrease in the dose rate in accordance with the data presented in Fig. 6.

The difference in the dose rate decrease for VSC-24 and SC-21 is caused by different contributions of individual isotopes to the dose rate (see Fig. 7). For comparison, Fig. 8 shows the changes in the dose rate, produced by SNF neutrons (dash-curve), subject to the SNF storage time.

5. Conclusions

The characteristics of the external radiation of the casks for SNF storage by dry method are calculated with taking into account the possible change in the spatial distribution of SNF in the basket, caused by the destruction of the fuel rod cladding. As an example, two storage casks are considered: concrete VSC-24 and metal SC-21. The change in the fluxes of neutrons and γ-quanta at a decrease in the height of the zone, filled by SNF in the basket, is shown. The long-lived isotopes ^{90}Y (^{90}Sr), ^{106}Rh (^{106}Ru), ^{134}Cs, ^{137m}Ba (^{137}Cs), ^{144}Pr (^{144}Ce), ^{154}Eu and ^{60}Co are considered to be the main emitters of γ-quanta. ^{244}Cm is considered as a neutron emitter.

Table 3
Gamma dose rates per source particle of each of the six main SNF isotopes on the side surfaces of VSC-24 and SC-21 storage casks.

Storage cask (N detector)	No	Scenario	^{154}Eu	^{134}Cs	^{137}Cs	^{144}Pr	^{106}Rh	^{90}Y
			D·10^{19}, Sv/s 1γ					
VSC-24 (det-2)	1	24 SFA, normal	**7.17**	**0.609**	**0.082**	**135.8**	**2.53**	**130.0**
	2	24 SFA, 50% destr.	3.93	0.386	0.063	74.4	1.62	72.2
	3	10 SFA, 50% destr.	7.31	0.696	0.064	137.0	2.49	130.2
SC-21 (det-1)	4	21 SFA, normal	**26.8**	**3.09**	**1.31**	**257**	**2.73**	**288**
	5	21 SFA, 50% destr.	20.4	2.18	0.33	253	3.88	333
	6	9 SFA, 50% destr.	7.82	0.44	0.029	268	2.99	274

Table 4
Doses per source particle produced by^{60}Co isotope on the side surface of VSC-24 and SC-21 storage casks.

Storage cask (detector)	No	Scenario	^{60}Co D·10^{19}, Sv/s 1γ
VSC-24 (det-3)	1	24 SFA, normal	**542**
	2	24 SFA, 50% destr.	371
	3	10 SFA, 50% destr.	535
SC-21 (det-3)	4	21 SFA, normal	**321**
	5	21 SFA, 50% destr.	3.0
	6	9 SFA, 50% destr.	314

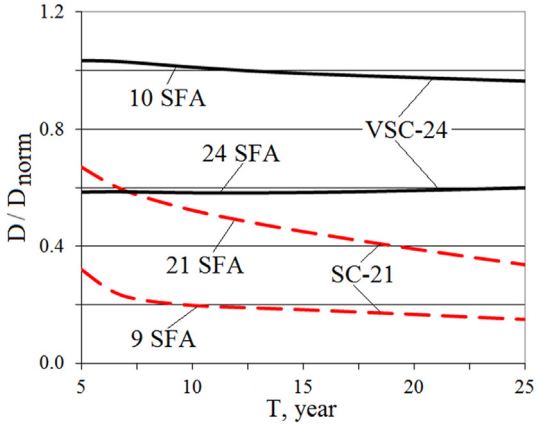

Fig. 6. The dependences of D(T)/D(T)$_{norm}$ on time for storage casks VSC-24 (I-24 and II-10) and SC-21 (I-21 and II-9).

The decrease of γ-quanta fluxes with time is determined by the half-lives of long-lived SNF isotopes. The characteristic time of the neutron flux decrease is determined by the half-life of ^{244}Cm: $T_{1/2} = 18.1$ years. The difference in the dependences of the external γ-radiation dose rate on time for the VSC-24 and SC-21 storage casks

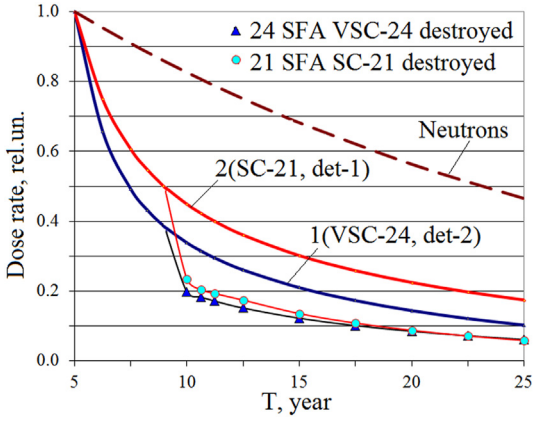

Fig. 8. Dose rates, produced by the external radiation of SNF γ-quanta in VSC-24 (curve 1, det-2) and SC-21 (curve 2, det-1) storage casks, versus storage time under normal operation and their change under the destruction of the fuel rod claddings (triangles - for VSC-24, and circles - for SC-21).

is explained by different attenuation and absorption of the primary radiation of SNF isotopes.

It is brought out clearly that a stepwise change in the dose rate of neutrons or γ-quanta, detected in the process of periodic measurements, indicates the destruction of the fuel rod claddings. The areas of the cask surface are determined, where the change in the dose rate, produced by neutrons or γ-quanta, is maximum at the decrease in the height of the area filled by SNF. Thus, the places, where the detectors should be installed to determine the integrity of the fuel rod claddings by the proposed method, are indicated.

Declaration of competing interest

The authors declare that they have no known competing financial interests or personal relationships that could have appeared to influence the work reported in this paper.

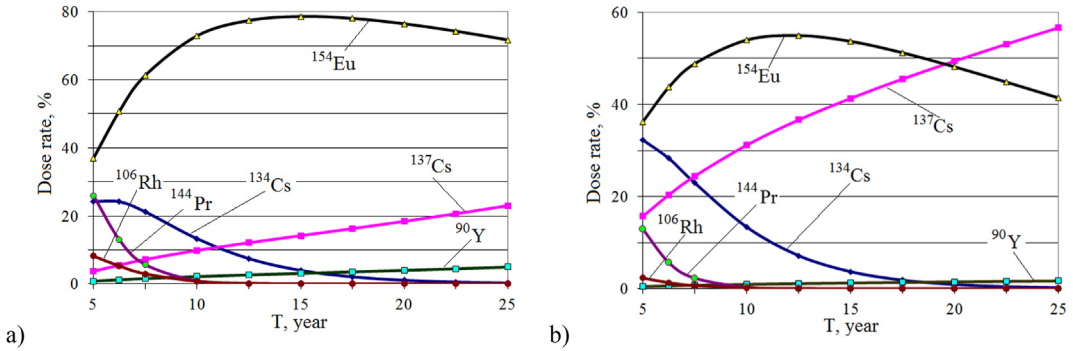

Fig. 7. (a) Contributions to the dose rates from individual isotopes versus time of SNF storage in VSC-24 cask (det-2). (b) Contributions to dose rates from individual isotopes versus time of SNF storage in the SC-21 cask (det-1).

References

[1] O.K. Chopra, et al., Managing Aging Effects on Dry Cask Storage Systems for Extended Long-term Storage and Transportation of Used Fuel – Revision 1, FCRD-UFD-2013-000294 30, 2013. ANL-13/15, September.

[2] S. Alyokhina, Thermal state of ventilated storage container with spent nuclear fuel under normal operation, Int. J. Nucl. Energy Sci. Technol. 13 (No.4) (2019) 381–398, https://doi.org/10.1504/IJNEST.2019.106056.

[3] S.V. Alyokhina, Naukovi Osnovy Teplovoyi Bezpeky Sukhoho Zberihannya Vidprats'ovanoho Yadernoho Palyva: Dys. Na Zdobuttya Nauk. Stupenya Doktora Tekhn. Nauk: Spets. 05.14.14 ≪Teplovi Ta Yaderni Enerhoustanovky ≫ – Odesa, 2019. – 302 s. (in Ukrainian).

[4] I.I. Zalyubovskii, S.A. Pismenetskii, V.G. Rudychev, et al., External radiation of a container used for dry storage of spent VVER-1000 nuclear fuel from the Zaporozhie Nuclear Power Plant, Atom. Energy 109 (6) (2011) 396–403.

[5] Tae-Man Kim, Myung-Hwan Seo, et al., Shielding analysis of dual purpose casks for spent nuclear fuel under normal storage conditions, Nucl. Eng. and Technol. 46 (4) (2014) 547–556.

[6] X-5 Monte-Carlo Team, MCNP-A General Monte-Carlo N-Particle Transport Code. Version 5. Volume I: Overview and Theory, Los Alamos National Laboratory, USA, 2003. LA-UR-03-1987.

[7] I.I. Zalubovsky, S.A. Pismenetskiy, V.G. Rudychev, et al., Protective structures for storing spent nuclear fuel from the Zaporozhye NPP, Atom. Energy 112 (4) (2012) 261–268.

[8] V.G. Rudychev, M.O. Azarenkov, I.O. Girka, et al., Contribution of radionuclides to heat release in the process of SNF dry storage, Probl. Atom. Sci. Technol. (2017) 91–96. No. 2 (108). Series: Physics of Radiation Effect and Radiation Materials Science (109).

[9] V.M. Kolobashkin, et al., Radiation Characteristics of Spent Nuclear Fuel, Handbook, Energoatomizdat, Moscow, 1983, pp. 167–169 (in Russian).

[10] R. Douglas, N. Ansslin, S. Hastings, et al., Passive Non-destructive Analysis of Nuclear Materials. M.: "Binom", 2000.

[11] P.M. Rinard, G.E. Bosler, J.R. Phillips, Calculated Neutron Source Spectra from Selected Irradiated PWR Fuel Assemblies, Los Alamos National Laboratory, USA, 1981. LA-9125-MS.

[12] V.G. Rudychev, N.A. Azarenkov, I.O. Girka, YeV. Rudychev, Identification of the fuel rod cladding destruction from the change of the SNF storage containers radiation//Problems of Atomic Science and Technology, Ser. Nucl. Phys. Investig. 5 (129) (2020) 111–119.

[13] V.G. Rudychev, N.A. Azarenkov, I.O. Girka et al., Method for Monitoring the Safety of Spent Nuclear Fuel Storage by Dry Method, Patent of Ukraine No. 120480 Dated 10.12.2019, Bul. No. 23.